FRACTURE OF A HIGH STRENGTH STEEL CONTAINING U-NOTCHES

F.J. Gómez, M. Elices and A. Valiente.

Departamento de Ciencia de Materiales, Universidad Politécnica de Madrid.
E.T.S.I. de Caminos, Canales y Puertos. Ciudad Universitaria, E-28040 - Madrid.

ABSTRACT

This paper presents a method to predict the failure load of U-notched bend specimens of a high strength, low toughness steel used in civil engineering. The prediction is based on the modelling of fracture as a cohesive cracking process. An experimental programme of three and four point bend fracture tests was performed to assess the method. The theoretical predictions were obtained by a finite element simulation of the tests, where a conventional elastoplastic constitutive equation and a two parameter softening curve were respectively used for the bulk material and for the cohesive zone. One of the two parameters, the fracture energy, was measured in independent fracture toughness tests involving precracked specimens, while the other, the cohesive strength, was determined by adjusting the numerically predicted load failure to the experimental value for one of the eight notch geometries examined. For the remaining seven, good agreement was found between the numerical and experimental failure loads.

INTRODUCTION

Some steels used in civil engineering are materials with an extremely high yield strength (above 1000 MPa) and a poor fracture toughness in contrast (below 50 MPa m$^{1/2}$) [1]. This lack of toughness generally involves low damage tolerance and entails a risk to the structural integrity that should be evaluated. When damage consists of the existence of cracks weakening a structural member made from these steels, the remaining bearing capacity can be predicted by means of well-known Fracture Mechanics theories, but there is no equivalent method to predict the failure load of members containing notches. This work explores the cohesive zone model as a tool to predict the failure load in such cases. It is a general approach that has been used to explain fracture from notches in PMMA [2].

In the cohesive zone model, fracture is viewed as a cracking process in which the cracked area is able to transmit stress as a function of the distance separating its faces. This function (the softening curve) is a material property and becomes null for a critical separation, marking the difference between the cohesive and non cohesive cracking. The softening curves considered in this work are the simplest ones, since they are defined by two material constants. Given that load failure predictions cannot be analytically derived from the cohesive model, it is implemented as an added feature of a finite element computer programme, so that the failure load of a number of notched bend specimens is numerically predicted. These predictions are compared with the values measured in fracture tests of specimens equal to those modelled in the calculations.

EXPERIMENTAL PROGRAMME

The material investigated in this work was a commercial, hot formed and air cooled eutectoid steel whose microstructure was formed by laminated pearlite colonies and round carbide. The chemical composition is

given in Table 1. The steel was supplied in 36-mm diameter bars and the specimens for all the mechanical tests were machined from the central part of the bars, with the largest dimension parallel to the bar axis.

The stress-strain curve shown in Fig. 1 was obtained from tensile and compressive testing. The yield tensile strength is approximately twice the yield compressive strength, the Bauschinger effect being very pronounced. Consequently, the strain hardening capacity in tension and compression is very different, as Fig 1 shows. The mechanical properties obtained from the stress-strain curve are given in Table 1. This table also includes the fracture toughness of the steel, measured according to ASTM E 399 [3] standard by using fatigue precracked bend specimens 16 mm thick.
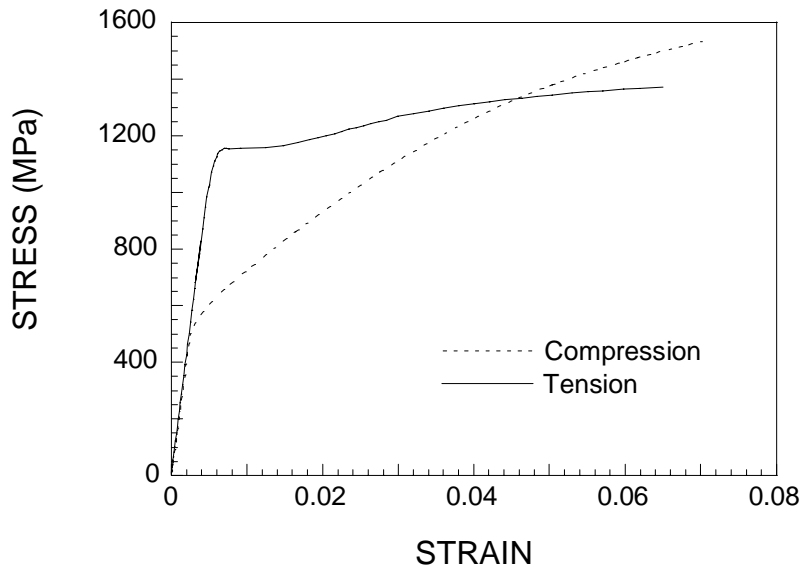
Figure 1: Tensile and compressive stress-strain curves of the tested steel.

TABLE 1

CHEMICAL COMPOSITION AND MECHANICAL PROPERTIES OF THE TESTED STEEL

C	0.65 %	Elastic modulus	208 GPa
S	0.70 %	Tensile yield strength	1143 MPa
Mn	1.20 %	Compressive yield strength	625 MPa
P	0.014 %	Tensile strength	1285 MPa
S	0.018 %	Maximum uniform elongation	6.7 %
V	0.25 %	Fracture toughness	33 MPam$^{1/2}$
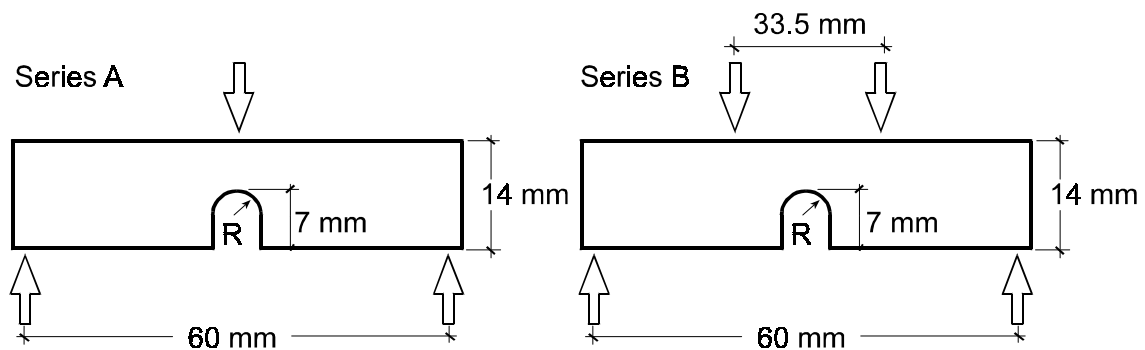
Figure 2: Notch geometries and bending devices of the two test series.

The fracture tests of notched specimens were performed by flexural loading of rectangular beams (7 mm thick, 14 mm wide and 60 mm long) containing U notches 7 mm deep at the middle cross section (Fig.2). The two test series included the same four notch radii (nominally, 0.1, 0.2, 0.5 and 1 mm) but differes in the

bending device. Four specimens nominally identical were tested for each test of the two series. The bending device of Series A was the three-point one of Fig 2, but in Series B it was changed to the four-point one of Fig 2.

The specimens were notched by two different procedures: electroerosion for the notch radii of 0.5 and 1 mm, and mechanical cutting by a diamond wire for the notch radii of 0.1 and 0.2 mm. Since the cohesive model is very sensitive to the notch geometry [2], the depth and specially the radius of each notch were carefully measured before testing by means of a profile projector at low magnification. Table 2 gives the mean values and the scatter for the four specimens nominally of the same geometry.

TABLE 2

MEASURED DIMENSIONS OF THE NOTCHED SPECIMENS

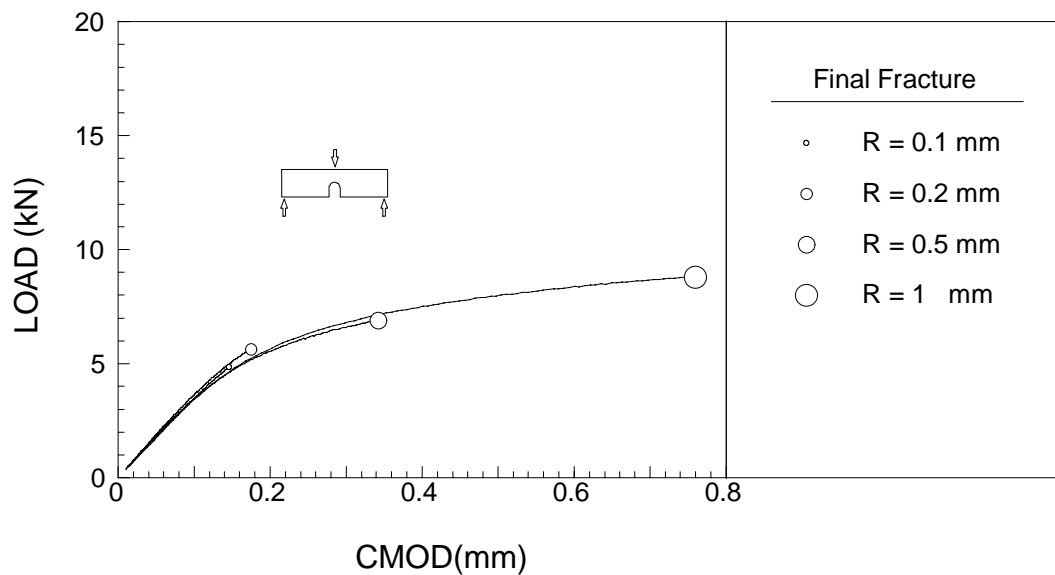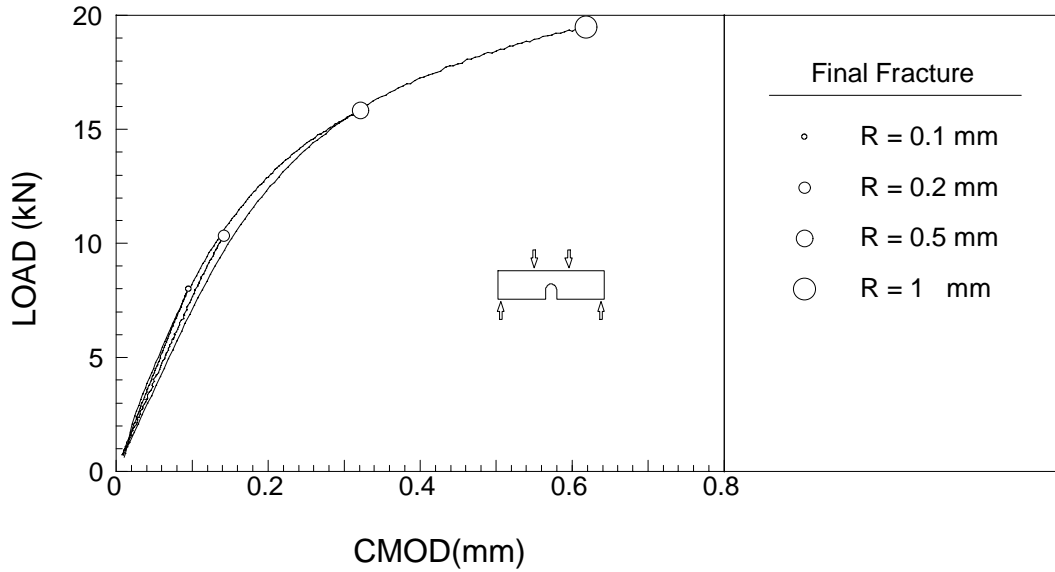| Series A		Series B	
R (mm)	a (mm)	R (mm)	a (mm)
0.101±0.001	7.0±0.3	0.106±0.004	6.84±0.09
0.171±0.006	7.0±0.2	0.171±0.005	7.09±0.06
0.505±0.002	6.96±0.04	0.498±0.002	6.98±0.01
1.00±0.01	6.96±0.06	1.000±0.002	7.00±0.03

Figure 3: Load-CMOD curves obtained in the fracture tests of notched specimens (Series A).

TABLE 3

MEASURED FAILURE LOAD OF THE TESTED NOTCHED SPECIMENS

Series A		Series B	
Notch radius	Failure load	Notch radius	Failure load
0.1 mm	8.9±0.1 kN	0.1 mm	16.90±0.06 kN
0.2 mm	7.1±0.2 kN	0.2 mm	14.20±0.03 kN
0.5 mm	5.1±1.3 kN	0.5 mm	11.1±1.6 kN
1 mm	5.1±1.0 kN	1 mm	9.8±2.1 kN

The tests were made by imposing a constant crack mouth opening displacement rate (CMOD control), which was measured by a strain gauge extensometer attached to the face of the specimen where the notch ended.

The Load-CMOD curve was recorded up to final fracture in each test. Fig. 3 and 4 show these curves for one of the four repeated tests and Table 3 gives the measured failure load with the experimental scatter.

Figure 4: Load-CMOD curves obtained in the fracture tests of notched specimens (Series B).

THEORETICAL BACKGROUND

The cohesive zone model was introduced in 1960s by Barenblatt [4] and Dugdale [5] to model the material response to the crack elastic stress singularity, but the current formulation is due to Hillerbourg [6] who generalized the model to account for the fracture of uncracked solids. Generally, the cohesive crack theory is applied to quasi-fragile materials such as concrete or ceramics [7], but recently it has been extended to polymeric and metallic materials such as PMMA [2] and aluminium [8].

In this theory, fracture is viewed as a cracking process that initiates at the point where the maximum principal stress σ_I reaches the cohesive strength f_t, a material constant. This crack consists of a displacement discontinuity surface inside the material that propagates perpendicularly to the direction of σ_I .The cracked area is able to transmit stress between its faces as a function $\sigma = f(w)$ of the normal displacement discontinuity w. This occurs up to a critical value w_c from which the transmitted stress vanishes, the cracked area able to transmit stress is the cohesive crack, and the cracking process transforms from cohesive into real for normal displacement discontinuities greater than w_c.

The function

$$\sigma = f(w) \tag{1}$$

is a material property called the softening curve that becomes null for $w > w_c$ and whose value at the origin is f_t ($f(0) = f_t$). The area enclosed under the softening curve:

$$G_F = \int_0^{w_c} f(w)dw \tag{2}$$

is the fracture energy G_F, since it coincides with the value of the energy release rate G that produces the brittle fracture of a cracked solid of the cohesive material [9]. The softening curves assumed in this work to predict failure loads are the rectangular functions $f(w) = f(0) = f_t$ for $0 \bullet w < w_c$ and $f(w) = 0$ for $w > w_c$. Despite being the simplest ones they have been satisfactorily used for other materials [2, 8]. These curves are determined by the two values that represent the sides of the rectangle, the cohesive strength f_t and the critical displacement w_c, or alternatively by one of the sides and the area, namely, the cohesive strength f_t and the

fracture energy G_F. The value of G_F can be experimentally found from a plain strain fracture toughness test of the cohesive material, where the brittle fracture of a precracked specimen occurs. The plain strain fracture toughness K_{Ic}, the elastic modulus E, the Poisson´s ratio ν and the fracture energy G_F can be related with the aid of the J integral when calculated at fracture along a contour surrounding the crack tip and not passing through the cohesive crack [9]. The relationship is:

$$G_F = (1-\nu^2)\frac{K_{Ic}^2}{E} \tag{3}$$

It has been shown [10] that this brittle behaviour of a cohesive material in a fracture toughness test requires specimens with all the dimensions roughly one order of magnitude greater than a characteristic length of the material, l_{ch}, defined as:

$$l_{ch} = \frac{EG_F}{f_t^2} \tag{4}$$

NUMERICAL PREDICTIONS

With a few exceptions, the cohesive model does not allow the analytical determination of the stress and strain field, so in practice, finite element calculations incorporating the cohesive cracking are necessary to predict failure loads on the basis of this theory. For the U–notched specimens of the steel tested in this work, a finite element commercial programme Abaqus [11] was used, with special elements in the ligament of the notch to allow the cohesive cracking. The loading and geometrical mirror symmetry facilitates the task of complementing the finite element calculation method with the cohesive cracking, since the cracking path is known to follow the symmetry plane.
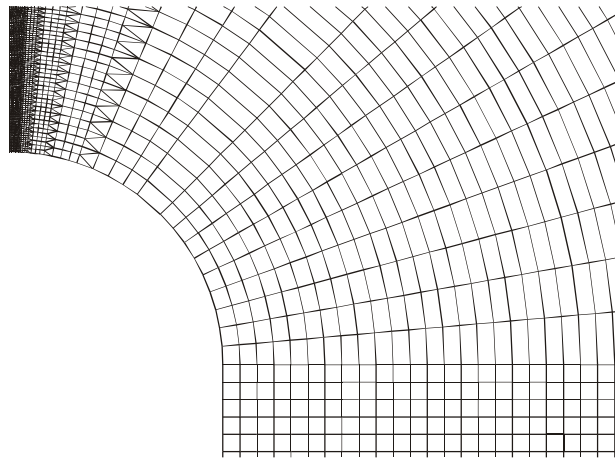

**Figure 5:** Type of finite element mesh used to apply the cohesive model to bend U–notched specimens.

The type of finite element mesh employed in the calculations is depicted in Fig 5. It was only necessary to construct the mesh of a half of each specimen due to the mirror symmetry. The elements used for the bulk material were conventional, linear, plane strain elements with four integration points. The size of the elements ranged from 5 μm at the notch root to 0.4 mm far from the notch. The constitutive equation adopted for the bulk material was that of a conventional elastic-plastic material obeying the Von Mises yield criterion and having the strain hardening and the Bauschinger effect shown by the stress-strain curve of Fig 1.

The special elements used for reproducing the cohesive cracking were one-dimensional with two nodes and no initial length. They were placed along the specimen ligament, at the symmetry plane, with a node joined to the plane but free to move on it, and the other shared with the bulk elements of the contiguous layer. A user material subroutine was specifically developed to integrate the special elements into the general finite element mesh. The length of the special elements can increase, giving rise to an attractive force between the nodes which depends on the element length. This dependence, the constitutive equation of the especial

elements, was obtained from the softening curve by transforming the cohesive stresses into nodal forces of the special elements by the usual procedure in the finite element method. The CMOD control of the tests was reproduced in the numerical calculations by using the non-linear algorithm that allows the length of the arc force-cohesive displacement curve to be controlled [12] at each loading step.
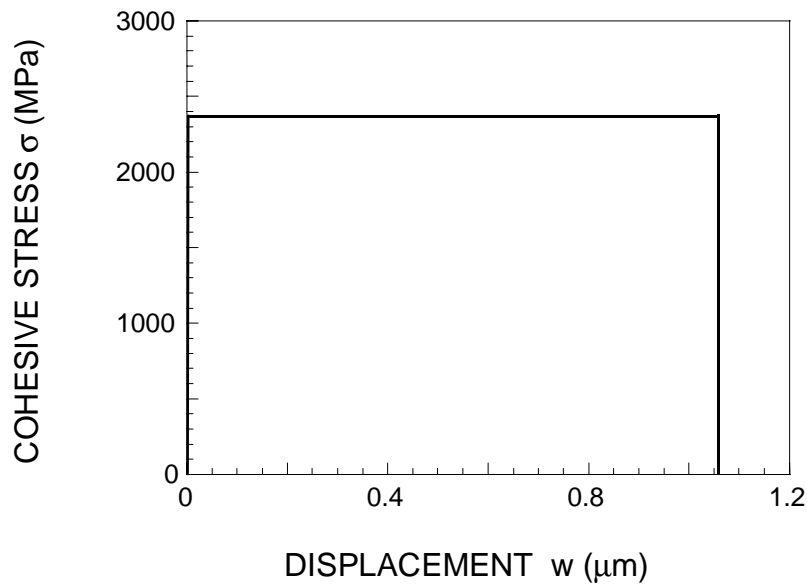
Figure 6: Softening curve of the tested steel.
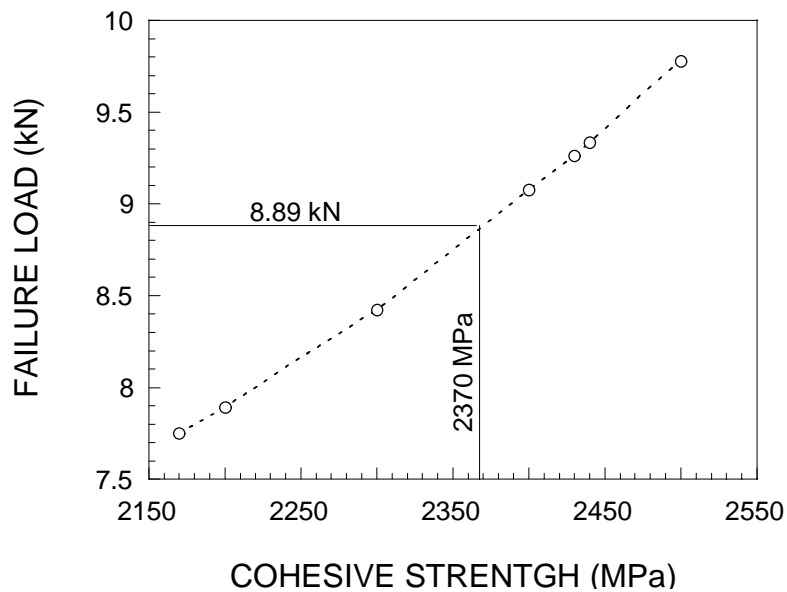
Figure 7: Determination of the cohesive strength for the tested steel.

The softening curve finally used is that shown in Fig. 6. Since Abaqus does not allow a strictly rectangular curve, a slightly trapezoidal rather than rectangular curve was used in fact, but the difference was meaningless. This curve was derived from the fracture energy and the cohesive strength of the tested steel (the area and the height of the rectangle). The fracture energy is 5.00 kJ/m², according to Eq (3) and the data given in Table 1, but no formula relating the cohesive strength f_t to other mechanical properties is available. It was determined from an experimental failure load, that of the specimens of Series A with the largest notch radius. The numerical failure load for this bending device and notch radius was calculated by making the cohesive strength range from 2100 MPa to 2500 MPa. This failure load is plotted in Fig 7 as a function of the cohesive strength. The numerical failure load is seen to coincide with the experimental one at a cohesive strength of 2370 MPa, so this value was adopted for the tested steel.

Once the softening curve was found, the finite element programme with cohesive cracking was applied to the remaining seven notch configurations of Series A and B. To account for the deviation of the real notch depth from the nominal one, all the calculations were performed for two values of this dimension, 0.94a and 1.04a, a being the nominal crack depth. The computed failure loads are shown in Table 4 jointly with the deviation due to this uncertainty as to the notch depth. An example of the load-CMOD curves numerically obtained (three point bend, 1 mm notch radius) is shown in Fig 8.

TABLE 4
CALCULATED FAILURE LOAD OF THE TESTED NOTCHED SPECIMENS

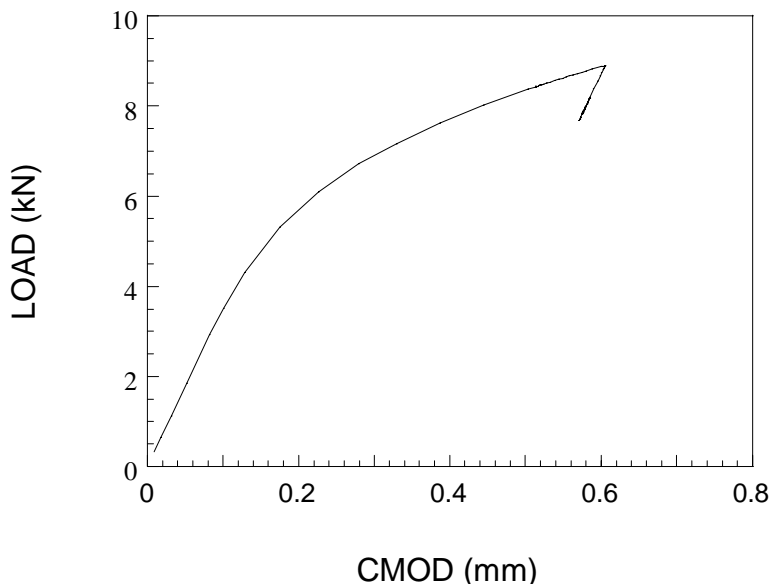| Series A		Series B	
Notch radius	Failure load	Notch radius	Failure load
0.1 mm	8.9±0.7 kN	0.1 mm	18.3±1.3 kN
0.2 mm	7.4±0.6 kN	0.2 mm	15.2±1.0 kN
0.5 mm	5.7±0.4 kN	0.5 mm	12.0±0.9 kN
1 mm	5.0±0.4 kN	1 mm	10.6±0.8 kN

Figure 8: A load-CMOD curve numerically obtained.

DISCUSSION OF RESULTS

The experimental values and the numerical predictions of the failure load of the tested U-notched specimens were plotted in Fig 9 as a function of the notch radius, for comparison. The numerical values are the band bounded by the couple of solid lines, since each one corresponds to one of the notch depths considered in the calculations (the upper line corresponds to the shorter notch and the bottom line to the longer one). The experimental values are plotted as points, the bars being the experimental scatter. In all the cases these error bars meet the uncertainty band of the numerical predictions, so theory and experiments agree.

CONCLUDING REMARKS

It has been shown that the cohesive zone model provides reliable values for the failure load of a high strength, low toughness steel containing U-notches. This is supported by the experimental results obtained with four notch radii and two types of loading. Further, the cohesive model requires only two material constants, one of them measured in independent tests and the other obtained as a fitting parameter of the

theory to different experiments. To obtain the theoretical predictions, the cohesive cracking model was incorporated into a commercial finite element programme.
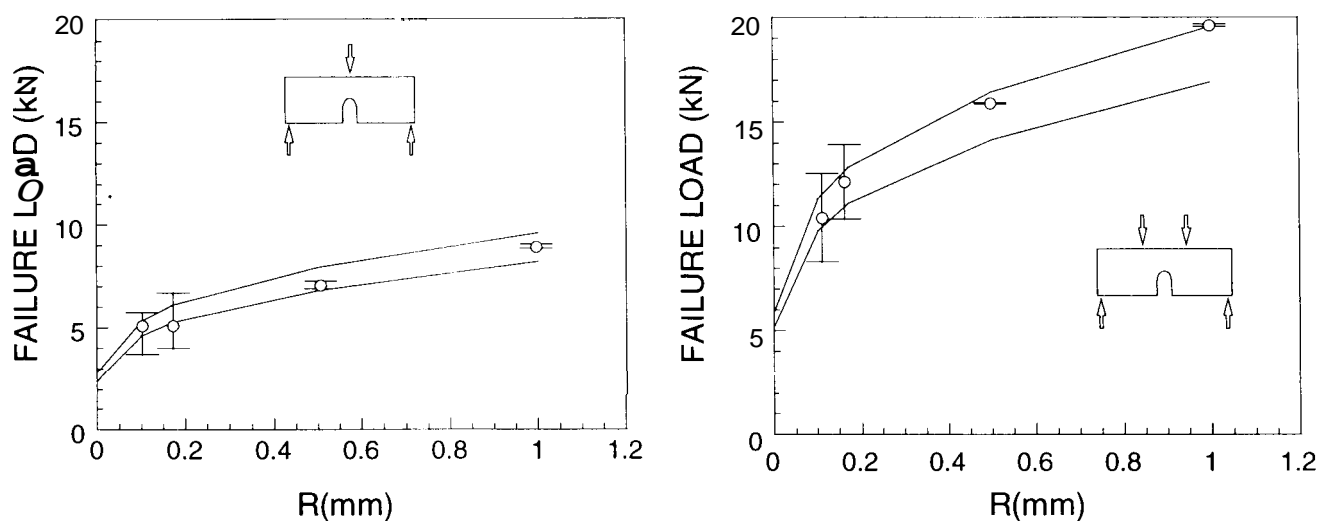
Figure 9: Experimental and numerically predicted failure loads
for the bend tested U-notched specimens.

ACKNOWLEDGMENTS

REFERENCES

1. Valiente, A. and Elices, M. (1998), Engineering Failure Analysis, **5,** 219.

2. Gómez, **F.** J., Elices, M. and Valiente, A. (2000), Cracking in PMMA containing U-shaped notches, Fatigue and Fracture Engineering Materials and Structures (In press).

3. American Society of Testing and Materials (1983), ASTM E399 Standard, ASTM, Philadelphia (USA).

4. Barenblat, G.I. (1962), Advanced Applied Mechanics. **7,***55.*

5. Dugdale, D.S. (1960), Journal of Mechanics and Physics of Solids **8,** 100.

6. Hillerbourg, A.H., Modéer, M. and Petersson, P.E. (1976), Cement and Concrete Research 6,773.

7. Elices, M., and Planas, J. (1996), Advanced Ceramics Based Materials **4,** 1 16.

8. Lin, G., Cornec, A. and Schwalbe, K.H. (1998), Fatigue and Fracture Engineering Materials and Structures, **21,** 1159.

9. Rice, J., (1968) Mathematical Analysis in the Mechanics of Fracture, in Fracture: An Advanced Treatise, **H.** D. Liebowitz, ed., Pergamon, New York (USA).

10. Planas, J. and Elices, M. (1992), International Journal of Fracture **55,** 153

11. Abaqus (1997) Abaqus/standard user's manual, Version *5,* Hibbit, Karlsson & Sorensen Inc.

12. Crisfield, M.A. (1995) Non-linear finite element analysis of solids and structures. Vol 1, John Wiley & Sons, Chichester (UK).